

JURNAL TEKNIK PERTANIAN LAMPUNG

ISSN 2302-559X (print) / 2549-0818 (online)

Journal homepage: https://jurnal.fp.unila.ac.id/index.php/JTP



Enhancing Sustainability in Packaging: Response Surface Optimized Sago Pith Waste Biocomposites with PBAT and MDI

Maya Irmayanti¹, Sarifah Nurjanah²,⊠, Akbar Hanif Dawam Abdullah³, Rossy Choerun Nissa³, Yeyen Nurhamiyah³

- ¹ Master Program Agroindustrial Technology, Faculty of Agro-Industrial Technology, Universitas Padjadjaran, West Java, INDONESIA.
- ² Department of Agricultural and Biosystem Engineering, Faculty of Agro-Industrial Technology, Universitas Padjadjaran, West Java, INDONESIA.
- ³ Research Center for Biomass and Bioproducts, National Research and Innovation Agency, West Java, INDONESIA.

Article History:

Received: 24 July 2024 Revised: 21 December 2024 Accepted: 31 December 2024

Keywords:

Biocomposite, Chain extender, Melt-mixing, Response Surface Methodology, Sago pith waste.

Corresponding Author:

Sarifah@unpad.ac.id
(Sarifah Nurjanah)

ABSTRACT

This study aims to optimize the biocomposites of sago pith waste (SPW) for sustainable packaging applications. The biocomposite was prepared using the biodegradable polymer polybutylene adipate-co-terephthalate (PBAT) as a matrix and methylendifenyl disocyanate (MDI) as a chain extender. RSM-CCD was used to assess the impact of the incorporation of SPW (5-20% p/p) and MDI (1-5%) into the PBAT matrix on the tensile strength and elongation of biocomposites by melt mixing. The optimal formula shown by RSM was 5% SPW and 5% MDI, which resulted in a 5.14 MPa tensile strength and 8.14% elongation. The barrier properties of all treatments, including moisture content, contact angle, and water absorption, were checked. The optimal formula showed good barrier properties compared to other treatments: water content of 3.12%, contact angle of 42.84°, and water absorption of 0.82%. Other characterizations of SEM, FTIR, DSC, TGA, and biodegradability tests showed an increase in SPW-PBAT compatibility due to the use of MDI. MDI as a chain extender had a positive impact on the material's strength, and the addition of SPW accelerated the degradation process, thus improving biodegradability.

1. INTRODUCTION

Plastics are versatile materials that play important roles in daily life. Their widespread use is due to their lightweight, durability, malleability, bio-inertness, hydrophobicity, and low-cost properties (Bishop *et al.*, 2020). In 2016, global plastic production was 335 million tons, which increased to 367 million tons by 2022 (Plastics Europe, 2021). Fossil-based plastics present notable environmental challenges, as a substantial portion (approximately 40%) of this waste accumulates in landfills and threatens marine ecosystems, with research showing high toxicity to aquatic organisms (Venkatachalam & Palaniswamy, 2020). The escalating issue of plastic waste has prompted research on degradable materials as potential replacements for synthetic polymers, as these materials can naturally decompose into harmless byproducts (Guimarães *et al.*, 2022).

PBAT (Polybutylene Adipate Terephthalate) has a high elongation value, indicating excellent flexibility and ease of processing, which facilitates its widespread use (Liu *et al.*, 2021). PBAT is biodegradable within a few weeks, making it an environmentally friendly alternative (Scaffaro *et al.*, 2019). PBAT can be used in food packaging applications because of these properties. However, PBAT's lackluster performance and high cost hinder its widespread adoption in packaging (Cai *et al.*, 2018; Moustafa *et al.*, 2017).

Natural fibers have gained significant interest as replacements for synthetic counterparts in engineering applications (Gapsari et al., 2021). Research suggests the potential of SPW (Sago Pith Waste) as a novel biocomposite filler (Azura et al., 2017). Sago starch production generates SPW as a by-product with SPW produced around 15% of total wet weight (Istikowati et al., 2021; Siruru et al., 2019). Current practices often involve discharging this waste into rivers, leading to environmental pollution of waterways and the surrounding ecosystems (Rashid et al., 2018). Despite its waste designation, SPW retains a significant amount of lignocellulose fibers (23-40% cellulose, 9.2-14.5% hemicellulose, and 3.9-7.5% lignin) (Fauziah et al., 2020; Siruru et al., 2019). This high lignocellulosic content makes SPW a promising candidate for development as a biocomposite filler. The application of SPW as a reinforcing filler in PVA-based biocomposites has been investigated. Toh et al. (2011) demonstrated that the dry mixing method yielded biocomposites with the most favorable mechanical properties (tensile strength of 4.85 MPa) but compromised water resistance.

MDI (Methylendifenly Diisocyanate) is commonly used to enhance the compatibility of many materials. High reactivity with carboxyl and hydroxyl groups is imparted by its molecular structure, which is characterized by two isocyanate functional groups (Pan *et al.*, 2018). Tensile strength and elongation break improved by 1.9 and 6.8 times, respectively, when 2% compatibilizer was added to bamboo flour (BF)/PBAT composites (Xie *et al.*, 2020). According to Li *et al.* (2021), tensile strength increased significantly from 4.55 MPa to 6.52 MPa when 1% MDI was added to starch/PBAT.

RSM is a common practice in the pursuit of optimal results, in which the influence of different independent variables is analyzed to inform the design of an optimal solution (Albooyeh *et al.*, 2022). The application of RSM offers several advantages, particularly in terms of reducing the number of planned experiments and rapidly identifying the optimal parameters including those about the interaction of each variable (Belaadi *et al.*, 2020; Benzannache *et al.*, 2021).

As far as author aware, no study has been conducted to assess the potential benefits of SPW/PBAT with MDI couplers in the production of biodegradable materials. This study aimed to optimize the mass ratio of SPW, PBAT, and MDI through melt-mixing to achieve enhanced tensile strength and elongation at break. The resulting biocomposite barrier characteristics, such as moisture content, contact angle, and water absorption were also assessed. SEM, FTIR, DSC, TGA, and biodegradability tests were used to further characterize the neat polymer, low, and optimal formulation.

2. MATERIALS AND METHODS

2.1. Materials

SPW was sourced from PT. Bangka Asindo Agri, Bangka Belitung. PBAT was obtained from Shijiazhuang Tuya Technology (China). MDI was obtained from BASF (NCO content 31%, Germany).

2.2. Experimental Design and Optimization for SPW and MDI-Based Biocomposite

The focus was on optimizing two key variables: the sago pith waste concentration (% w/w) and MDI concentration (% w/w). Meanwhile, the PBAT concentration (% w/w) was adjusted by keeping the total percentage concentration of the mixture three components at 100% for each run. Tensile strength and elongation were chosen as the response variables for optimization within the RSM-CCD model. Table 1 presents a detailed overview of the model variables, including their coded and actual values and Table 2 presents the run code and composition of each run.

2.3. Methods

SPW (size 60 mesh), PBAT, and MDI were melt-mixed using a HAAKE Polylab OS system Rheomix at 120°C and 80 rpm for 10 minutes, according to RSM ratios. Table 2 outlines the specific compositions of the prepared biocomposites. The resulting biocomposite chunks were molded on a YASUDA brand mini test press at 120°C, resulting in the production of sago pith waste biocomposite sheets.

Table 1. The actual values and coding levels of the central composite design that correspond to the design

Variable		Range and Levels	
variable	-1	0	1
X1-Sago pith waste (%)	5.00	12.50	20.00
X2-MDI (%)	1.00	3.00	5.00

Table 2. Run code and composition of three variables in each run

Run	Sago Pith Waste (% w/w)	MDI (% w/w)	PBAT (% w/w)
1	5.00	5.00	90.00
2	12.50	3.00	84.50
3	1.89	3.00	95.11
4	12.50	3.00	84.50
5	12.50	0.17	87.33
6	12.50	3.00	84.50
7	5.00	1.00	94.00
8	12.50	5.83	81.67
9	12.50	3.00	84.50
10	12.50	3.00	84.50
11	20.00	5.00	75.00
12	20.00	1.00	79.00
13	23.11	3.00	73.89

2.4. Characterization of the Biocomposites

2.4.1. Mechanical Properties (Tensile Strength and Elongation)

The biocomposite sample tensile strength and elongation were measured in compliance with ASTM D3039. Using a die cutter, dumbbell-shaped specimens were prepared, and micrometers were used to quantify their thicknesses. A Universal Testing Machine (UCT-5 T, Orientec Co. Ltd, Japan) was used for mechanical testing.

2.4.2. Barrier properties

Moisture content was analyzed using a moisture analyzer (KERN & Sohn, Germany). The method used to calculate the water absorption capacity was ASTM D570-22. Water absorption capacity was calculated using Equation 1.

Water absorption capacity =
$$\frac{W_t - W_o}{W_o} \times 100$$
 (1)

where W_o represent the initial weight and W_t represent the final weight of the sample.

The contact angle was measured using $\pm 5~\mu L$ of water droplets on the biocomposite surface. The static contact angle was calculated by taking measurements at three separate spots on the surface biocomposite. The contact angle was then captured using a mobile phone and processed with ImageJ software.

2.4.3. Characterization of RSM Low and Optimal Condition

Further testing was conducted on RSM Low and Optimal conditions. These conditions are based on the highest and lowest elongation values in the RSM treatment. A scanning electron microscope (Merk Jeol) was used for Morphological investigation. Samples were photographed at 500x magnification under a 10 kV electron beam voltage. It was recorded as an example of projection on the monitor screen.

The functional group's spectra were collected using the FTIR (Fourier Transform Infrared Spectroscopy) 4000 spectrometer (Perkin Elmer., Waltham, MA, USA) with 64 scans in the spectral range from 4000 to 280 cm⁻¹.

A DSC Polyma instrument is used for DSC (Differential Scanning Calorimetry) analysis. Heated at a rate 20 mL/min under nitrogen atmosphere, with a heating rate of 20°C/min and the temperature range is 20°C to 300°C. PerkinElmer TGA equipment is used to assess samples' thermal stability through TGA (Thermogravimetric Analysis). Mass loss was monitored as the temperature increased from 40 to 600°C at a heating rate of 10°C/min.

A modified ASTM G21 standard was used to assess biodegradability and salt agar (SA) medium was used by Nissa *et al.* (2019). Using ImageJ software, the amount of fungal growth on the samples was evaluated after the 21-day incubation period.

3. RESULTS AND DISCUSSION

3.1. Model Data Adequacy Assessment

To validate the mathematical model created by RSM-CCD, Table 2 compares predicted response values to actual experimental data. The model's statistical significance was determined using analysis of variance (ANOVA).

The RSM model predicted and actual tensile strength and elongation values are compared in Figure 1. The diagonal line's close clustering of data points suggests a good connection between actual and predicted responses, corroborating the accuracy of the model. This alignment supports the validity of the RSM technique and is in line with Dixit & Yadav (2019) findings.

Table 3. Design and	d experiment result	s utilizing RSM base	ed on actual an	d predicted values
---------------------	---------------------	----------------------	-----------------	--------------------

	Range of Actual Va	riable	Actual and Predicted Value of Resp				
D	Sago Pith	MDI (%	Tensile Strength (MPa)		Elongation (%)		
Run	Waste (% b/b)	b/b)	Predicted Value	Actual Value	Predicted Value	Actual Value	
1	5.00	5.00	5.26	5.14	8.30	8.14	
2	12.50	3.00	4.63	4.78	4.61	4.31	
3	1.89	3.00	4.13	3.89	8.17	8.58	
4	12.50	3.00	4.88	4.63	4.61	4.89	
5	12.50	0.17	3.00	3.50	2.69	2.87	
6	12.50	3.00	4.63	4.87	4.61	5.00	
7	5.00	1.00	2.95	2.94	4.92	4.50	
8	12.50	5.83	6.26	5.87	5.34	5.15	
9	12.50	3.00	4.68	4.63	4.61	4.57	
10	12.50	3.00	4.63	4.45	4.61	4.26	
11	20.00	5.00	6.31	6.56	3.26	3.68	
12	20.00	1.00	4.01	4.01	2.90	3.07	
13	23.11	3.00	5.38	5.14	3.18	2.76	

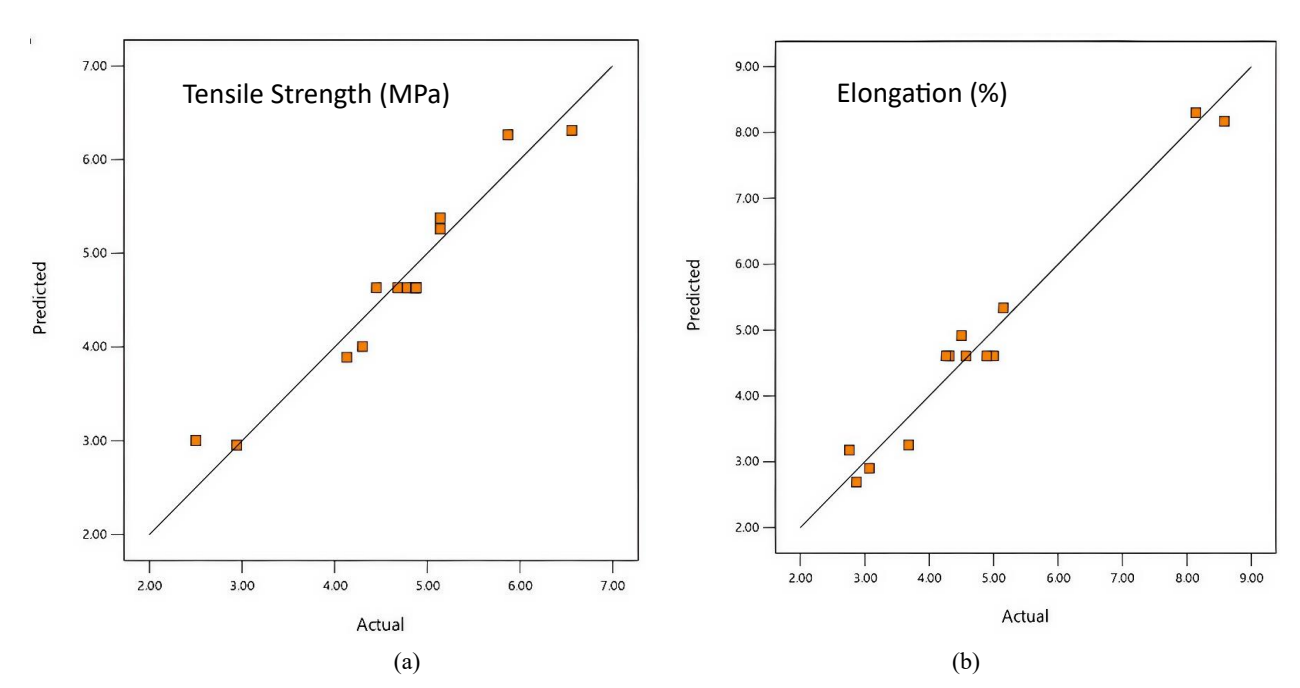


Figure 1. Relationship between actual and predicted values of the model (a) tensile strength; (b) elongation

3.2. RSM and Anova Analysis for SPW Biocomposite

3.2.1. Effect of variables on tensile strength

To evaluate each variable's impact on the response, a linear model was constructed using the data shown in Table 3. Equation 2 describes the RSM model developed for biocomposite tensile strength.

$$Y = 2.03 + 0.07 x_1 + 0.58 x_2 \tag{2}$$

where x_1 represents SPW and x_2 represents MDI, the ANOVA findings in Table 4 show a p-value is less than 0.05, this indicates the coefficients of the statistical significance, confirming that both SPW and MDI have a significant impact on tensile strength. As such, the relationship between these factors and the response is well captured by the RSM model.

ANOVA validated the RSM model's reliability. A high regression coefficient (R²=0.94) and the minimal difference between adjusted and predicted R² (<0.2) indicate a strong correlation between predicted and observed tensile strength. The relationship between the tensile strength of the resultant biocomposite and the concentration of MDI and SPW is shown in Figure 2. The plot shows a positive association between MDI concentration and tensile strength, implying that increasing MDI content results in higher tensile strength. On the other hand, there was a negative relationship between tensile strength and SPW concentration. Adding lignocellulosic fillers like SPW to the thermoplastic matrix (PBAT) may not always increase the biocomposite tensile strength (Hejna et al., 2020). MDI can potentially prevent crack formation during tensile strength testing, thereby leading to improved mechanical properties (Xie et al., 2020).

Table 4. Tensile Strength of SPW/PBAT/MDI Biocomposites from the CCD Model: An ANOVA Analysis

Source	Sum of Squares	df	Mean Square	F-value	p-value	
Model	12.85	2	6.43	74.86	< 0.0001	significant
X1-Sago Pith Waste	2.21	1	2.21	25.79	0.0005	
X2-MDI	10.64	1	10.64	123.94	< 0.0001	
Residual	0.86	10	0.09			
Lack of Fit	0.73	6	0.12	3.89	0.1	not significant
Pure Error	0.13	4	0.03			
Cor Total	13.71	12				
Std.Dev	0.29		\mathbb{R}^2	0.94		
Mean	4.63		Adjusted R ²	0.92		
C.V %	6.32		Predicted R ²	0.87		
		Adequate precision		23.86		

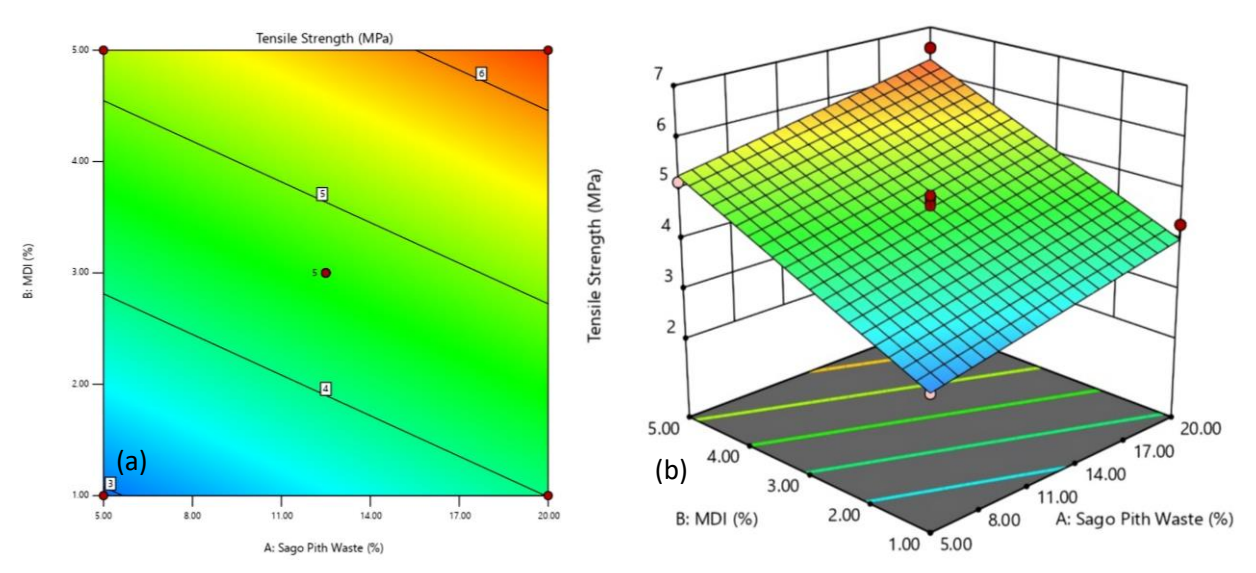


Figure 2. Two variable effects on tensile strength: (a) Contour plot, and (b) Three-dimensional response surface

3.2.2. Effect of variables on elongation

Based on the data in Table 4, multiple regression analysis was used to create a second-order quadratic model. The biocomposite elongation RSM model is represented by Equation 3.

$$Y = 5.07 - 0.32 x_1 + 1.54 x_2 - 0.05 x_1 x_2 + 0.01 x_1^2 - 0.07 x_2^2$$
(3)

0.97

0.94

0.83

19.45

The interaction terms in the equation are denoted by x_1x_2 , while the squared terms are represented by x_1^2 and x_2^2 . According to the ANOVA results, every coefficient has a statistically significant (p<0.05).

The ANOVA analysis (Table 5) showed a significant model (p<0.05) with a high F-value (41.23), indicating a good fit for predicting elongation values. The strong regression correlation coefficient (R^2 = 0.97) supported this. A three-dimensional plot of the independent factors and the biocomposite elongation value is shown in Figure 3. The elongation value decreased with increasing SPW concentration and the elongation value increased with increasing MDI concentration. The decrease in the elongation value that occurs with increasing SPW concentration is due to the lignocellulose content in SPW. Biocomposite may exhibit brittle fracture behavior if the filler content is increased without sufficient adhesion modification (Barczewski *et al.*, 2018).

Source	Sum of Squares	df	Mean Square	F-value	p-value	
Model	37.13	5	7.43	41.23	< 0.0001	significant
X1-Sago Pith Waste	24.92	1	24.92	138.36	< 0.0001	
X2-MDI	6.98	1	6.98	38.77	0.0004	
X1X2	2.30	1	2.30	12.74	0.0091	
X1 ²	1.98	1	1.98	11.01	0.0128	
$X2^2$	0.6100	1	0.6100	3.39	0.1083	
Residual	1.26	7	0.18			
Lack of Fit	0.82	3	0.27	2.45	0.20	not significant
Pure Error	0.44	4	0.11			
Cor. Total	38.39	12				

 R^2

Adjusted R2

Predicted R2

Adeq Precision

Table 5. Elongation of SPW/PBAT/MDI Biocomposites from the CCD Model: An ANOVA Analysis

0.42

4.75

8.93

Std. Dev

Mean

C.V %

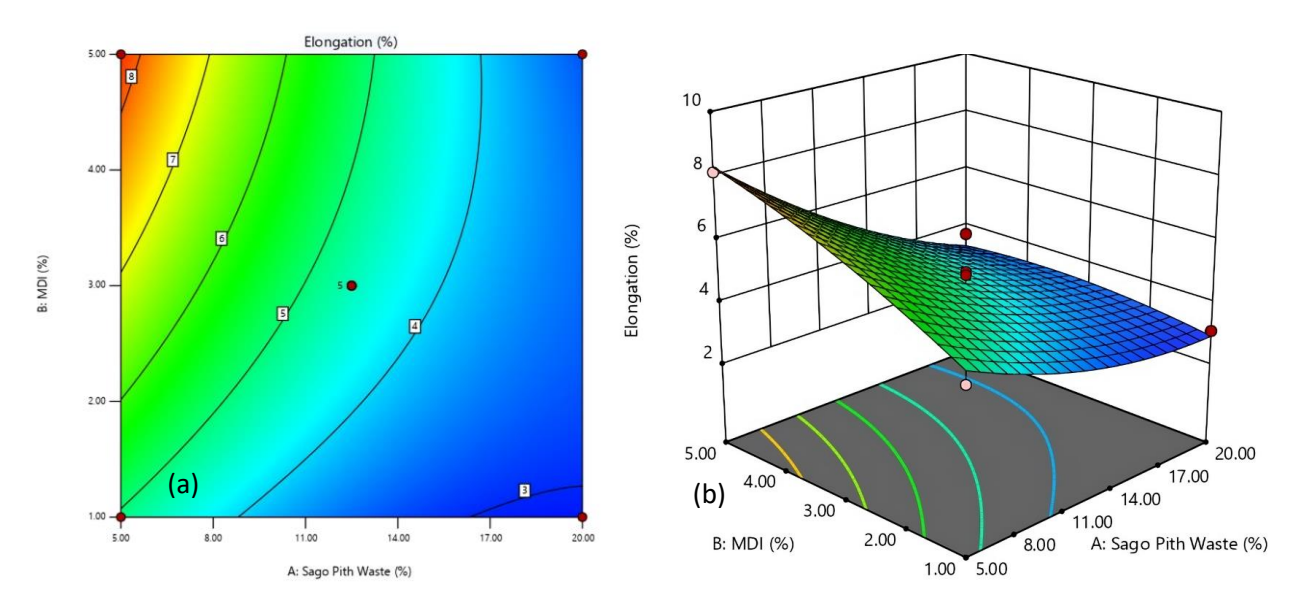


Figure 3. Two variable effects on elongation: (a) Contour plot, and (b) Three-dimensional response surface

3.3. Optimization of the RSM-CCD Model

CCD model's predictive capabilities, an experiment was conducted using the optimized concentrations of SPW and MDI (both 5%). The model predicted a tensile strength of 5.26 MPa and elongation of 8.30%. Tensile strength and elongation of the optimized biocomposite by experimental results were 5.14 MPa and 8.14, respectively. A comparison between the actual and predicted results for both responses showed a nearly linear relationship, indicating the accuracy of the model fit (Song *et al.*, 2011).

3.4. Barrier Properties

The investigation into the barrier properties of biocomposites was conducted on all RSM treatments, yet it was not incorporated into the RSM response. The test encompassed the assessment of water content, contact angle, and water absorption. The rationale behind this investigation was to ascertain the capacity of biocomposites to impede moisture absorption (ALP, 2020).

3.4.1. Moisture and contact angle test

Figure 4a shows the moisture contents and contact angles of the biocomposite samples. The biocomposite samples' moisture content and contact angle changed between the RSM treatments (3.10 - 4.00% moisture content, $18 - 43^\circ$ contact angle). Treatment 5 (RSM Low) exhibited the highest moisture content (3.98%) and the lowest contact angle (18.37%), whereas treatment 1 (RSM optimal) displayed the lowest moisture content (3.12%) and the highest contact angle (42.84°) . This indicates that a negative correlation between the moisture content and contact angle-lower moisture content corresponds to a higher contact angle, and vice versa.

The contact angle of all treatments was lower than that of neat PBAT (70°) (Rasyida *et al.*, 2017), which was likely due to the addition of SPW. The moisture content measurements revealed an increase. The inclusion of MDI increased contact angle, consistent with prior research where MDI-modified biocomposites displayed higher contact angles compared to those with HDI or TDI hexamethylene diisocyanate (HDI) and toluene diisocyanate (TDI) (Hejna *et al.*, 2023) owing to reduced polarity.

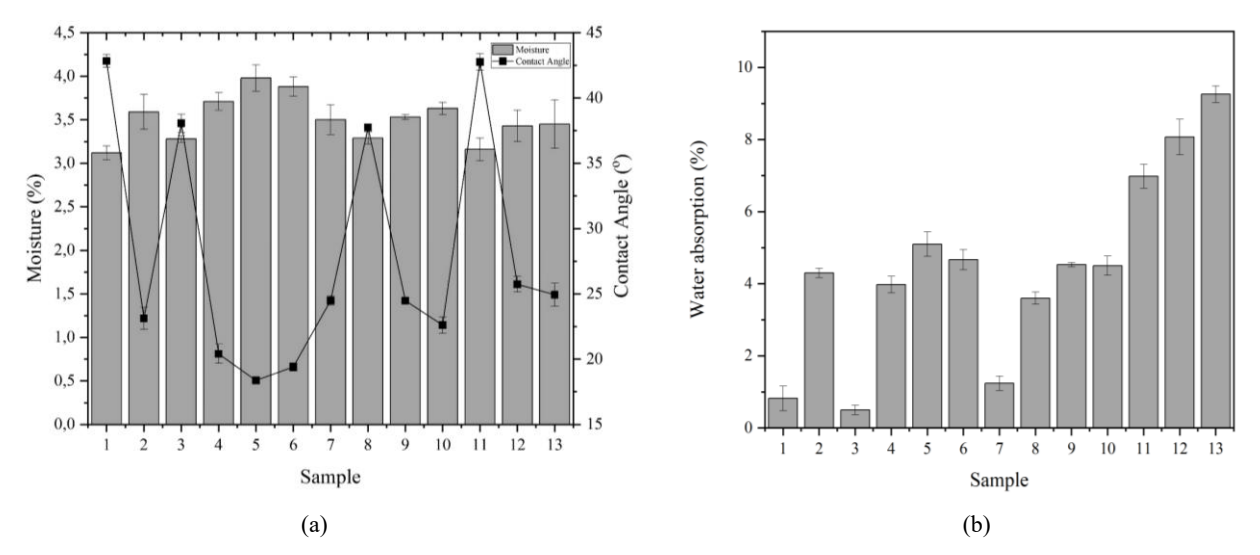


Figure 4. (a) Moisture content and contact angle, (b) Absorption of the sample

3.4.2. Water absorption test

The water absorption of the 13 RSM treatments is shown in Figure 4b, which exhibited varying levels of water absorption. Treatments 3 and 1 (RSM optimum) had the lowest water absorption value with values of 0.050 and 0.82%, respectively. In contrast, treatment 13 containing the highest SPW content of 23.11%, exhibited the highest water

absorption at 9.26%. This is due to the fact that SPW is a semi-crystalline polymer with low crystallinity and is sensitive to moisture (Yee *et al.*, 2011). Increasing SPW concentration also causes the free –OH groups in the cellulose and hemicellulose structure to absorb water through hydrogen bonds formed between water molecules and OH groups (Fabian *et al.*, 2023). This causes high water absorption in treatments with high SPW concentration.

3.5. Characterization of the Optimized Sago Pith Waste Biocomposite

3.5.1. SEM

Figure 5 shows the cross section of neat PBAT, RSM low, and RSM optimal. The surface of the neat PBAT appeared relatively smooth and lacked visible defects, indicating a good surface structure. RSM optimal exhibited a homogeneous and smooth surface, indicating a more even distribution of SPW particles within the PBAT matrix. Furthermore, the 5% MDI in RSM optimal improved adhesion between SPW and PBAT, as evidenced by fewer gaps. This suggests a stronger bonding between the filler and PBAT matrix. Conversely, RSM low shows more voids in the biocomposite, potentially explaining its lower mechanical properties compared to RSM optimal. Reinforcing this notion, Lai *et al.* (2014) observed voids in biocomposites with high SPW content, attributing it to low compatibility and resulting in poor tensile properties. These findings suggest that reducing SPW concentrations while increasing MDI concentrations improves the interaction between filler and matrix, leading to a smoother surface and enhanced mechanical properties of the biocomposites. The urethane bond resulting from the reaction of isocyanate groups forming MDI can increase the interfacial bond between SPW and PBAT polymer matrix (Seo *et al.*, 2020). Thus, with increasing MDI concentration the interfacial bond between SPW and PBAT polymer matrix can be improved.

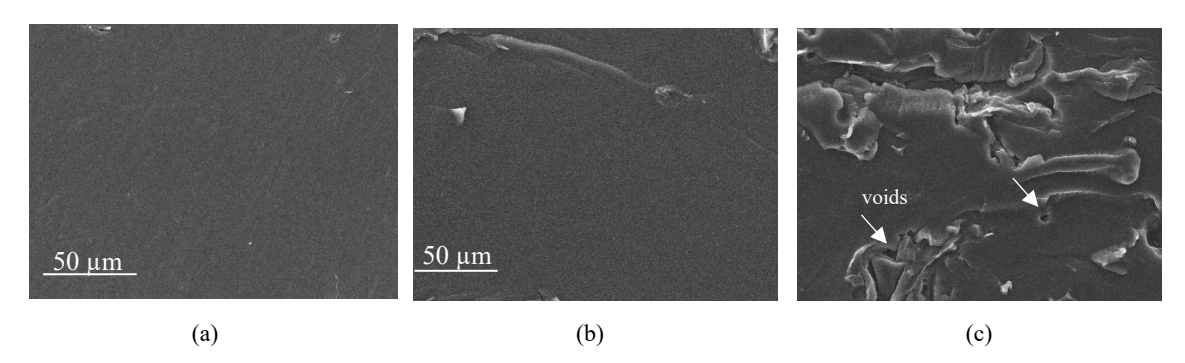


Figure 5. Cross-section morphology at 500x magnification (a) Neat PBAT; (b) RSM Optimal; (c) RSM Low

3.5.2. FTIR

Figure 6a shows the FTIR spectra used to study the molecular structures of neat PBAT, RSM Low, and RSM optimal. The presence of carbonyl ester groups in neat PBAT spectra at 1708 cm⁻¹ (C=O stretching) and 1240 cm⁻¹, respectively (Mahata *et al.*, 2020). The peak at 2960 cm⁻¹ indicated PBAT contains methyl and methylene bonds (Almond *et al.*, 2020). The introduction of SPW and MDI into the RSM treatments led to additional peaks and spectral changes. RSM optimal spectrum shows a new peak at 3276 cm⁻¹ indicating hydrogen bonding between SPW and PBAT matrix. Furthermore, a new peak at 2158 cm⁻¹, corresponding to isocyanate linkages (N=C=O), which usually appears at 2100-2275 cm⁻¹ (Khazabi & Sain, 2014). In contrast, RSM low exhibits weaker interactions or fewer hydrogen bonds, as evidenced by the absence of the new peak observed in RSM optimal and minimal changes around 3411 cm⁻¹ (characteristic of hydroxyl groups). Both RSM low and optimal spectra show the presence of hydroxyl groups (~3300 cm⁻¹), indicating polysaccharides (cellulose and hemicellulose) from SPW, which are absent in neat PBAT (Hejna *et al.*, 2023).

3.5.3. DSC

The DSC thermogram in Figure 6b shows the melting behavior of neat PBAT and RSM modified biocomposites. Neat PBAT exhibits a melting point (Tm) of 120°C, while the RSM treatments (low and optimal) display higher Tm values of 129.5°C and 131.4°C, respectively. This increase in Tm for the RSM modified samples indicates enhanced thermal

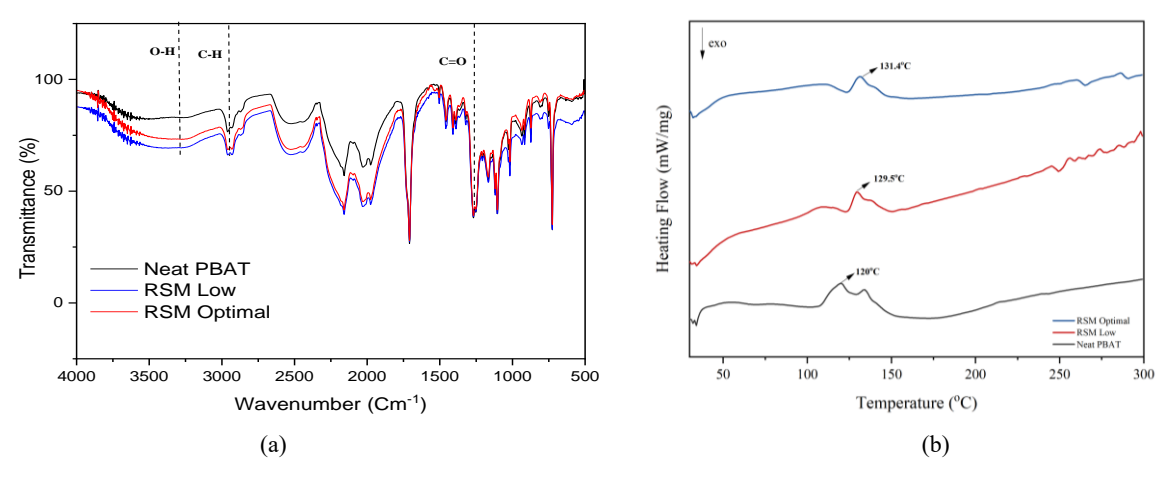


Figure 6. (a) FTIR of polymeric biocomposite, (b) DSC of polymeric biocomposites

stability compared to neat PBAT. Additionally, RSM optimal shows a higher heat flow, signifying a more pronounced endothermic process compared to the other samples. The lower endothermic peak observed in RSM low compared to the optimal RSM suggesting a less significant thermal event.

3.5.4. TGA and DTG

Figure 7 shows the TGA and DTG curves. The curves can be divided into four sections, corresponding to the decomposition of different material components at various temperatures. All treatments exhibited minimal weight loss (1-3%) between 100-300°C, indicating thermal stability. This initial weight loss is likely due to moisture evaporation from the natural fiber (SPW) (Rajeshkumar *et al.*, 2021). Neat PBAT starts significant weight loss around 300°C, followed by RSM low at a slightly higher temperature. RSM optimal treatments exhibit the latest degradation onset, indicating improved thermal stability. During the decomposition phase (400-500°C), neat PBAT experienced the fastest weight loss, while RSM optimal decomposed gradually and retained more weight compared with RSM low. The residual weight after 500°C suggests incomplete decomposition, with RSM optimal showing the highest value. This could be explained by the homogeneous distribution of SPW in the RSM optimal PBAT matrix, which is consistent with Dixit & Yadav (2019) that better adhesion between BPSF and the polymer matrix can result in better thermal stability.

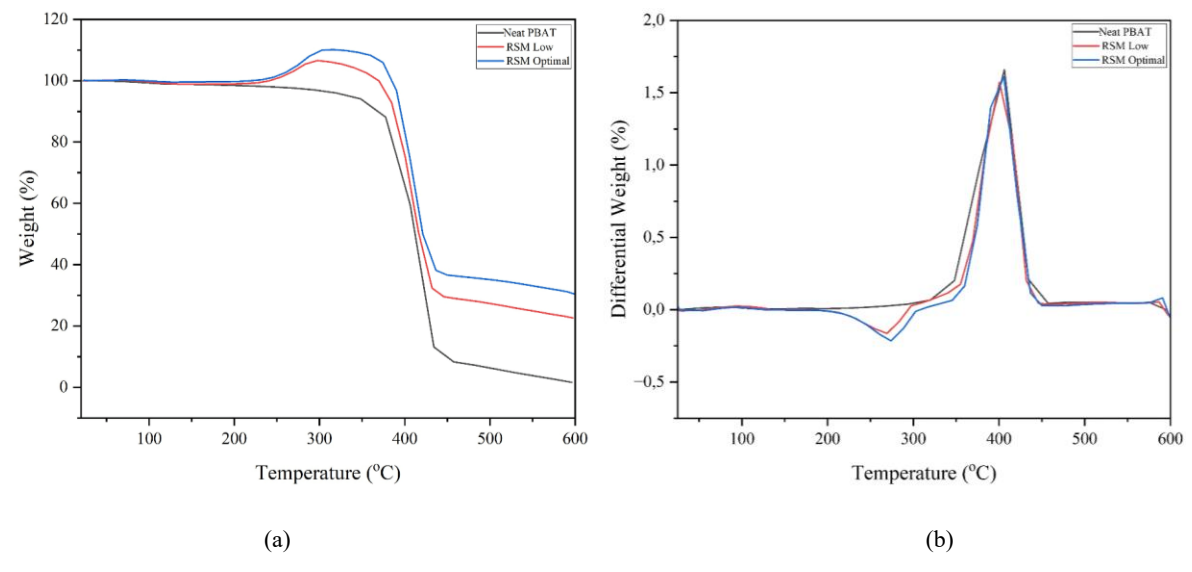


Figure 7. (a) TGA, and (b) DTG of polymer biocomposites

987

 Sample
 Neat PBAT
 RSM Low
 RSM Optimal

 0 day
 0%
 0%
 0%

 10 day
 51.80%
 45.65%

Table 6. The biodegradable test by A.niger at day 0 and day 10

3.5.5. Biodegradability Test

The biodegradation test results (Table 6) showed that the biocomposites from RSM low and optimal treatments exhibited higher degradation values than neat PBAT. RSM low treatment (51.80% degradation) was more readily degraded by A.niger fungus than RSM optimal (45.65%). This can be attributed to the higher concentration of SPW, which accelerated the degradation process of the resulting composite. Furthermore, the lower MDI concentration in RSM low compared optimal might also contribute to its faster degradation rate. Overall, both RSM low and optimal treatments showed higher degradation rates than neat PBAT. This aligns with previous research showing that the addition of lignocellulosic materials can improve the biodegradation of PBAT-based composites. The research conducted by Xu et al. (2019), who used reed fiber (RF) and MCC in their PBAT composites.

4. CONCLUSIONS

The formulation of SPW/MDI biocomposites using a PBAT matrix was successfully optimized by the use of RSM. The RSM identified 5% (b/b) SPW and 5% (b/b) MDI as the optimal concentrations for achieving the desired properties. Experimental results show that tensile strength and elongation optimal concentration are 5.14 MPa and 8.14%, respectively. A higher SPW content resulted in decreased barrier properties, while an increased MDI concentration led to enhanced barrier performance. SEM micrographs revealed the presence of more voids in the RSM low sample than optimal. FTIR analysis suggested stronger interactions between components in the RSM optimal than RSM low. The DSC and TGA results indicated superior thermal stability for RSM optimal. Finally, a biodegradability Test confirmed that SPW incorporation accelerated the degradation rate. In conclusion, the potential of SPW as a filler in PBAT-based biocomposites for environmentally sustainable packaging applications.

ACKNOWLEDGMENTS

The authors would like to thank the Bandung Advanced Characterization Laboratory for its facilities, and scientific, and technical support. We also thank the National Research and Innovation Agency of the Republic of Indonesia for their assistance with the BRIN Science e-service.

REFERENCES

Albooyeh, A., Soleymani, P., & Taghipoor, H. (2022). Evaluation of the mechanical properties of hydroxyapatite-silica aerogel/epoxy nanocomposites: Optimizing by response surface approach. *Journal of the Mechanical Behavior of Biomedical Materials*, *136*, 105513. https://doi.org/10.1016/j.jmbbm.2022.105513

Almond, J., Sugumaar, P., Wenzel, M.N., Hill, G., & Wallis, C. (2020). Determination of the carbonyl index of polyethylene and polypropylene using the specified area under band methodology with ATR-FTIR spectroscopy. *E-Polymers*, **20**(1), 369–381. https://doi.org/10.1515/epoly-2020-0041

- ALP (Associated Labels & Packaging). (2020). What Do Barrier Properties Do? https://associatedlp.com/news/2020/what-do-barrier-properties-do (Accessed at 23 May 2025)
- Azura, A.R., Adzami, N.S., & Tajarudin, H.A. (2017). Utilization of *Metroxylan sagu* pith waste as biodegradable filler for natural rubber (NR) latex films. *Solid State Phenomena*, **264**, 198–201. https://doi.org/10.4028/www.scientific.net/SSP.264.198
- Barczewski, M., Mysiukiewicz, O., & Kloziński, A. (2018). Complex modification effect of linseed cake as an agricultural waste filler used in high density polyethylene composites. *Iranian Polymer Journal*, 27, 677–688. https://doi.org/10.1007/s13726-018-0644-3
- Belaadi, A., Laouici, H., & Bourchak, M. (2020). Mechanical and drilling performance of short jute fibre-reinforced polymer biocomposites: Statistical approach. *International Journal of Advanced Manufacturing Technology*, *106*, 1989–2006. https://doi.org/10.1007/s00170-019-04761-4
- Benzannache, N., Belaadi, A., Boumaaza, M., & Bourchak, M. (2021). Improving the mechanical performance of biocomposite plaster/ Washingtonian filifira fibres using the RSM method. *Journal of Building Engineering*, 33, 101840. https://doi.org/10.1016/j.jobe.2020.101840
- Bishop, G., Styles, D., & Lens, P.N.L. (2020). Recycling of European plastic is a pathway for plastic debris in the ocean. *Environment International*, 142, 105893. https://doi.org/10.1016/j.envint.2020.105893
- Cai, X., Yang, X., Zhang, H., & Wang, G. (2018). Aliphatic-aromatic poly(carbonate-co-ester)s containing biobased furan monomer: Synthesis and thermo-mechanical properties. *Polymer*, *134*, 63–70. https://doi.org/10.1016/j.polymer.2017.11.058
- Fabian, D.R.C., Durpekova, S., Dusankova, M., Cisar, J., Drohsler, P., Elich, O., Borkova, M., Cechmankova, J., & Sedlarik, V. (2023). Renewable poly(lactic acid)lignocellulose biocomposites for the enhancement of the water retention capacity of the soil. *Polymers*, *15*(10), 2243. https://doi.org/10.3390/polym15102243
- Dixit, S., & Yadav, V.L. (2019). Optimization of polyethylene/polypropylene/alkali modified wheat straw composites for packaging application using RSM. *Journal of Cleaner Production*, 240, 118228. https://doi.org/10.1016/j.jclepro.2019.118228
- Fauziah, A.R., Lanuru, M., Syahrul, M., & Werorilangi, S. (2020). Utilization of solid waste from sago flour industry (sago pith waste) as biodegradable plastic. *Advances in Environmental Biology*, 14(1), 42–47. https://doi.org/10.22587/aeb.2020.14.1.7
- Gapsari, F., Purnowidodo, A., Hidayatullah, S., & Suteja, S. (2021). Characterization of Timoho fiber as a reinforcement in green composite. *Journal of Materials Research and Technology*, 13, 1305–1315. https://doi.org/10.1016/j.jmrt.2021.05.049
- Giri, J., Lach, R., Grellmann, W., Susan, M.A.B.H., Saiter, J.M., Henning, S., Katiyar, V., & Adhikari, R. (2019). Compostable composites of wheat stalk micro- and nanocrystalline cellulose and poly(butylene adipate-co-terephthalate): Surface properties and degradation behavior. *Journal of Applied Polymer Science*, 136(43), 1–11. https://doi.org/10.1002/app.48149
- Guimarães, M.R., Scatolino, M.V., Martins, M.A., Ferreira, S.R., Mendes, L.M., Lima, J.T., Junior, M.G., & Tonoli, G.H.D. (2022). Bio-based films/nanopapers from lignocellulosic wastes for production of added-value micro-/nanomaterials. *Environmental Science and Pollution Research*, 29(6), 8665–8683. https://doi.org/10.1007/s11356-021-16203-4
- Hejna, A., Barczewski, M., Kosmela, P., Mysiukiewicz, O., Tercjak, A., Piasecki, A., Saeb, M.R., & Szostak, M. (2023). Sustainable chemically modified mater-bi/poly(ε-caprolactone)/cellulose biocomposites: Looking at the bulk through the surface. *Research Square*. https://doi.org/10.21203/rs.3.rs-3064683/v1
- Hejna, A., Sulyman, M., Przybysz, M., Saeb, M.R., Klein, M., & Formela, K. (2020). On the correlation of lignocellulosic filler composition with the performance properties of poly(ε-caprolactone) based biocomposites. *Waste and Biomass Valorization*, 11(4), 1467–1479. https://doi.org/10.1007/s12649-018-0485-5
- Istikowati, W.T., Sutiya, B., Sunardi, S., & Sunardi, S. (2021). Utilization of sago waste as animal feed material in Pemakuan Laut Village, Sungai Tabuk, Banjar Regency, South Kalimantan. *PengabdianMu: Jurnal Ilmiah Pengabdian Kepada Masyarakat*, 6(2), 149–155. https://doi.org/10.33084/pengabdianmu.v6i2.1822
- Khazabi, M., & Sain, M. (2014). Morphological and physico-thermal properties of soy-based open-cell spray polyurethane foam insulation modified with wood pulp fiber. *Advances in Petroleum Exploration and Development*, 7(1), 1–6.
- Lai, J.C., Rahman, W.A.W.A., & Toh, W.Y. (2014). Mechanical, thermal and water absorption properties of plasticised sago pith waste. *Fibers and Polymers*, 15(5), 971–978. https://doi.org/10.1007/s12221-014-0971-8
- Li, C., Chen, F., Lin, B., Zhang, C., & Liu, C. (2021). High content corn starch/Poly (butylene adipate-co-terephthalate) composites with high-performance by physical-chemical dual compatibilization. *European Polymer Journal*, 159, 110737.

https://doi.org/10.1016/j.eurpolymj.2021.110737

- Liu, Y., Liu, S., Liu, Z., Lei, Y., Jiang, S., Zhang, K., Yan, W., Qin, J., He, M., Qin, S., & Yu, J. (2021). Enhanced mechanical and biodegradable properties of PBAT/lignin composites via silane grafting and reactive extrusion. *Composites Part B: Engineering*, 220, 108980. https://doi.org/10.1016/j.compositesb.2021.108980
- Mahata, D., Cherian, A., Parab, A., & Gupta, V. (2020). In situ functionalization of poly(butylene adipate-co-terephthalate) polyester with a multi-functional macromolecular additive. *Iranian Polymer Journal*, 29, 1045–1055. https://doi.org/10.1007/s13726-020-00860-2
- Moustafa, H., Guizani, C., Dupont, C., Martin, V., Jeguirim, M., & Dufresne, A. (2017). Utilization of torrefied coffee grounds as reinforcing agent to produce high-quality biodegradable PBAT composites for food packaging applications. *ACS Sustainable Chemistry and Engineering*, 5(2), 1906–1916. https://doi.org/10.1021/acssuschemeng.6b02633
- Nissa, R.C., Fikriyyah, A.K., Abdullah, A.H.D., & Pudjiraharti, S. (2019). Preliminary study of biodegradability of starch-based bioplastics using ASTM G21-70, dip-hanging, and soil burial test methods. *IOP Conference Series: Earth and Environmental Science*, 277, 012007. https://doi.org/10.1088/1755-1315/2777/1/012007
- Pan, H., Li, Z., Yang, J., Li, X., Ai, X., Hao, Y., Zhang, H., & Dong, L. (2018). The effect of MDI on the structure and mechanical properties of poly(lactic acid) and poly(butylene adipate-co-butylene terephthalate) blends. *RSC Advances*, 8, 4610–4623. https://doi.org/10.1039/c7ra10745e
- Plastics Europe. (2021). Plastics the fact 2021. Plastics Europe market research group (PEMRG) and conversio market & strategy GmbH, 1–34. https://plasticseurope.org/
- Rajeshkumar, G., Seshadri, S.A., Devnani, G.L., Sanjay, M.R., Siengchin, S., Maran, P.J., Al-Dhabi, N.A., Karuppiah, P., Mariadhas, V.A., Sivarajasekar, N., & Anuf, A.R. (2021). Environment friendly, renewable and sustainable poly lactic acid (PLA) based natural fiber reinforced composites A comprehensive review. *Journal of Cleaner Production*, *310*, 127483. https://doi.org/10.1016/j.jclepro.2021.127483
- Rashid, M.b.M.R., Mijarsh, M.J.A., Seli, H., Johari, M.A.M., & Ahmad, Z.A. (2018). Sago pith waste ash as a potential raw material for ceramic and geopolymer fabrication. *Journal of Material Cycles and Waste Management*, **20**, 1090–1098. https://doi.org/10.1007/s10163-017-0672-7
- Rasyida, A., Fukushima, K., & Yang, M-C. (2017). Structure and properties of organically modified poly(butylene adipate-coterephthalate) based nanocomposites. IOP Conference Series: Materials Science and Engineering, 223, 012023. https://doi.org/10.1088/1757-899X/223/1/012023
- Scaffaro, R., Maio, A., Sutera, F., Gulino, E.F., & Morreale, M. (2019). Degradation and recycling of films based on biodegradable polymers: A short review. *Polymers*, 11(4), 651. https://doi.org/10.3390/polym11040651
- Seo, Y-R., Bae, S-U., Gwon, J., Wu, Q., & Kim, B-J. (2020). Effects of methylenediphenyl 4,4'-diisocyanate and maleic anhydride as coupling agents on the properties of polylactic acid/polybutylene succinate/wood flour biocomposites by reactive extrusion. *Materials*, 13(7), 1660. https://doi.org/10.3390/ma13071660
- Siruru, H., Syafii, W., Wistara, I.N.J., & Pari, G. (2019). Characteristics of metroxylon rumphii (pith and bark waste) from Seram Island, Maluku, Indonesia. *Biodiversitas*, 20(12), 3517–3526. https://doi.org/10.13057/biodiv/d201208
- Song, M-M., Branford-White, C., Nie, H-L., & Zhu, L-M. (2011). Optimization of adsorption conditions of BSA on thermosensitive magnetic composite particles using response surface methodology. *Colloids and Surfaces B: Biointerfaces*, **84**(2), 477–483. https://doi.org/10.1016/j.colsurfb.2011.02.002
- Venkatachalam, H., & Palaniswamy, R. (2020). Bioplastic world: A review. *Journal of Advanced Scientific Research*, 11(3), 43–53. https://sciensage.info/index.php/JASR/article/view/505
- Xie, X., Zhang, C., Weng, Y., Diao, X., & Song, X. (2020). Effect of diisocyanates as compatibilizer on the properties of BF/PBAT composites by in situ reactive compatibilization, crosslinking and chain extension. *Materials*, 13(3), 806. https://doi.org/10.3390/ma13030806
- Xu, J., Feng, K., Li, Y., Xie, J., Wang, Y., Zhang, Z., & Hu, Q. (2024). Enhanced biodegradation rate of poly(butylene adipate-coterephthalate) composites using reed fiber. *Polymers*, 16(3), 411. https://doi.org/10.3390/polym16030411
- Yee, T.W., Sin, L.T., Rahman, W.A.W.A., & Samad, A.A. (2011). Properties and interactions of poly(vinyl alcohol)-sago pith waste biocomposites. *Journal of Composite Materials*, 45(21), 2199–2209. https://doi.org/10.1177/0021998311401073